Journal of Applied Polymer Science

Immobilization of cationic polyelectrolyte on polystyrene spheres and adsorption for model whitewater contaminants

He Xiao,[1] Beihai He,[2] Junrong Li[2]

[1]College of Materials Engineering, Fujian Agriculture and Forestry University, Fuzhou, China 350002

[2]State Key Laboratory of Pulp and Paper Engineering, South China University of Technology, Guangzhou, China 510641

Correspondence to: H. Xiao (E-mail: xiaohe_river@163.com)

ABSTRACT: Polystyrene (PS) spheres with cationic polyelectrolyte brushes were prepared by reversible addition-fragmentation chain transfer polymerization (RAFT) from cross-linked PS spheres. These PS spheres were subsequently modified by reaction with chloroacetyl chloride and S,S-Bis(α,α′-dimethyl-α″-acetic acid) trithiocarbonate to serve as macro chain transfer agents (macro-CTAs). Methacryloxyethyltrimethyl ammonium chloride (MAC) was then grafted from these macro-CTAs of PS spheres to obtain cationic PS spheres. FT-IR, ^{13}C-NMR, SEM, element analysis, and TGA techniques were applied to investigate and optimize the structure of PS spheres. The cationic PS spheres loading 1.35 mmol/g poly-MAC were used as absorbents for removal of polygalacturonic acid (PGA) and sodium ligninsulfonate (lignin-Na). Adsorption capacity of cationic PS spheres could reach 3 mg PGA/g and 24 mg lignin-Na/g, respectively. Moreover, adsorption isotherm data of PGA were described by Langmuir-Freundlich model, whereas lignin-Na conformed to Langmuir model. Kinetic studies suggested that dissolved substances (PGA and lignin-Na) could diffuse into the pores of cationic PS spheres. © 2015 Wiley Periodicals, Inc. J. Appl. Polym. Sci. **2015**, *132*, 42509.

KEYWORDS: polyelectrolytes; polystyrene; resins; synthesis and processing

Received 12 March 2015; accepted 17 May 2015

DOI: 10.1002/app.42509

INTRODUCTION

Dissolved and colloidal substances (DCS) in a papermaking system continuously accumulate with increasing utilization of recycling white water. These contaminants are derived from wood constituents such as lignin, hemicellulose and extractives, and functional and auxiliary additives such as pulping and bleaching agents, defoamers, dispersants, sizing agents, coating materials, and wet-end additives.[1,2] Accumulation of these substances lead to many serious problems, including increased foaming, scaling, and corrosion problems, slime and biological growth, deposits of extractive materials of the DCS on wires and felts, increased consumption of chemicals, and the poor physical properties of the paper produced.[3–5]

The conventional methods to control detrimental substances in whitewater are based on the chemical treatments mostly, which generally requires high charge densities and low molecular weight polymers, such as poly(dimethyl diallyl ammonium chloride) (poly-DADMAC), polyethylenimine (PEI), and polyvinylamine (PVA_m). The detrimental substances fixed on the fibers and fines are removed from whitewater.[6–8] However, the fixed DCS in the fiber mat may still impair the machine runnability, especially in the press section and drying section.[9,10] Other technologies, such as membrane filtration treatment[11] and biological enzyme[12] have been proposed, but adaptability and costs have restricted implementations in mills.

Adsorption is one of the most effective approaches to remove pollutants from systems. In recent years, contaminants adsorption on solid absorbents in a fluidized bed reactor has been proposed for DCS removal from whitewater in papermaking systems.[13,14] Ion exchange resin is one of the most effective choices to resolve these problems in paper mills and cardboard industries.[15] Regarding ion exchange resins, it is known that PS spheres are widely used as the matrix material because of its low price, accessible, and good mechanical strength.[16,17] The properties of ion exchange resin mainly depend on the architecture of the surface functional groups.[18,19] Fibrous polymer such as quaternary ammonium polyelectrolyte anchored to polystyrene spheres might exhibit exciting adsorption behavior. In such structure, flexibility and partial mobility of polyelectrolyte brushes are expected to provide rapid interaction with the target molecules. The most common methods for preparation of polystyrene spheres grafted with polyelectrolyte brushes can be summarized as: (a) photo-emulsion polymerization based on a

© 2015 Wiley Periodicals, Inc.

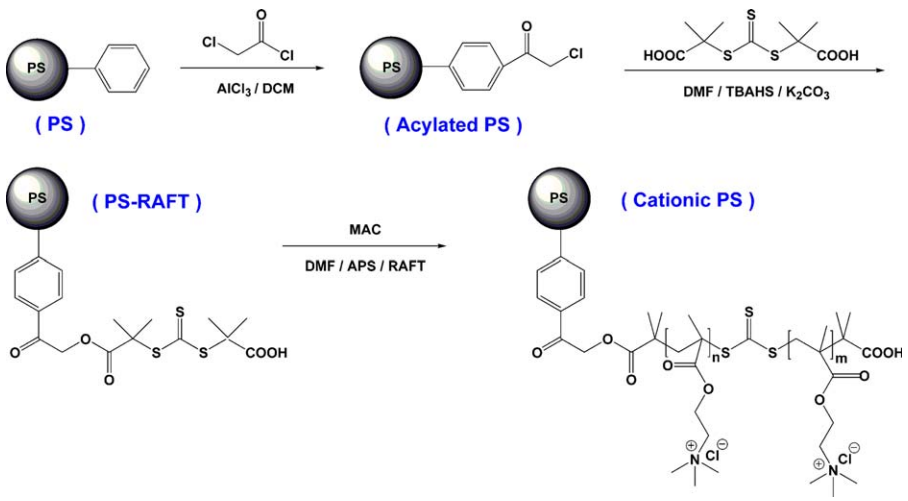

Figure 1. Schematic representation of synthetic route toward polystyrene spheres with cationic polyelectrolyte brushes. [Color figure can be viewed in the online issue, which is available at wileyonlinelibrary.com.]

grafting-from technique leading to a dense layer of chemically bound polyelectrolyte chains,[20] (b) controlled radical polymerization such as atom transfer radical polymerization (ATRP) and reversible addition-fragmentation chain transfer polymerization (RAFT),[21,22] and (c) self-assembly and micellar system.[23]

In the present work, PS spheres were first acylated by chloroacetyl chloride and then bonded with S,S-Bis(α,α′-dimethyl-α″-acetic acid) trithiocarbonate (RAFT agent) to serve as macro chain transfer agents (macro-CTAs). Poly-MAC was then initiated from these macro-CTAs of polystyrene spheres using ammonium persulfate as an initiator (Figure 1). Surface-initiated parameters (e.g., PS/MAC mass ratio, initiator, and RAFT agent concentration) were optimized to evaluate the results of polymerization of MAC on the surface of active PS spheres. Finally, adsorption of polygalacturonic acid (PGA) and sodium ligninsulfonate (lignin-Na) on the new cationic PS spheres was performed to study the potential of such resin to remove DCS from whitewater. A batch adsorption technique was used to determine adsorption isotherms and kinetics of model contaminants (PGA and lignin-Na) by the new resin.

EXPERIMENTAL

Materials

Polygalacturonic acid (PGA) (Aladdin) had a molecular weight between 25,000 and 50,000 and a purity higher than 90%. The stock solution was made by dissolving PGA in 0.1*M* NaOH during 24 h. This solution was then adjusted to pH 7 with HCl. Sodium ligninsulfonate (lignin-Na) (Aladdin) had a purity higher than 96% and was dissolved in deionized water to obtain a final solution. Cross-linked polystyrene spheres (PS spheres, 50–100 mesh) were kindly supported by Zhengguang Industrial Co., Zhejiang, China.

S,S-bis(α,α′-dimethyl-α″-acetic acid) trithiocarbonate (RAFT agent) was prepared according to a previously published method.[24] Dichloromethane (DCM) was dried with calcium hydride (CaH_2) overnight and distilled before use. Methacryloxyethyltrimethyl ammonium chloride (72% solution in water) was obtained from J&K Scientific without further purification. Anhydrous aluminum chloride, *N*,*N*-dimethyl formamide (DMF), chloroacetyl chloride, ammonium persulfate, tetrabutylammonium hydrogen sulfate (TBAHS), and potassium carbonate (K_2CO_3) were all of analytical grade.

Acylation of PS Spheres

A total of 2.08 g purified PS beads were suspended in 30 mL anhydrous dichloromethane and 4.52 g chloroacetyl chloride, followed by batch-wise addition of anhydrous aluminum chloride (5.82 g) with continuous stirring. The reaction solution was stirred at 30°C for 4 h and washed successively by tetrahydrofuran, dilute hydrochloric acid (volume ratio 1 : 25), distilled water, and methanol. Acylated PS spheres were obtained after 50°C vacuum drying until constant weight which was light yellow powder.

Incorporation RAFT Agent onto Acylated PS Spheres

Three grams of acylated PS spheres (containing 3.29 mmol/g active chlorine) was swelled in 60 g DMF for 12 h. Then, 3.29 g (11.67 mmol) RAFT agent, 3 g tetrabutylammonium hydrogen sulfate, and 3 g potassium carbonate were thrown into the mixture with continuous stirring at 80°C for 12 h. Finally, the acylated PS spheres loading RAFT agent to serve as macro-CTAs (PS-RAFT) were obtained by washed with ethanol, distilled water and methanol successively. The products were vacuum-dried at 50°C for 24 h to constant weight, which were collected as yellowish spherical beads.

Surface Initiated RAFT of MAC from PS Spheres

A total of 0.2 g macro-CTAs of PS spheres were suspended in 7.6 g DMF and swelled for 12 h. After that, 5.56 g MAC (72% solution in water) and 4 mg additional RAFT agent were added in the DMF mixtures. After nitrogen was bubbled through for at least 30 min, the polymerization system was heated to 65°C and kept for 20 h. The initiator ammonium persulfate (APS, 4 mg) was injected into the flask to initiate polymerization. The crude products were successively washed by distilled water, ethanol, and methanol and vacuum-dried at 50°C for 24 h to constant weight. The final products were yellowish spherical beads

Table I. Effect of PS/MAC Mass Ratio on Preparation of Cationic PS Spheres

Samples[a]	PS/MAC[b]	S %	N %	Weight increasing /%	RAFT loading (mmol/g)	Polyelectrolyte Loading (mmol/g)
PS-RAFT[c]	—	8.848	—	—	0.92	—
Cationic PS[d]	1 : 5	7.345	1.18	16.06	0.77	0.84
Cationic PS[d]	1 : 10	7.527	1.37	24.76	0.78	0.98
Cationic PS[d]	1 : 20	7.082	1.75	38.86	0.74	1.25
PS-RAFT[e]	—	4.806	—	—	0.50	—
Cationic PS[f]	1 : 5	4.141	1.03	12.47	0.43	0.74
Cationic PS[f]	1 : 10	4.226	1.21	18.43	0.44	0.86
Cationic PS[f]	1 : 20	3.787	1.45	28.94	0.39	1.04

[a] Monomer (MAC) concentration: 30%, solvent: DMF, APS concentration: 0.6%, additional RAFT concentration: 1%, polymerization temperature:70°C, polymerization time: 12 h.
[b] PS/MAC: the mass ratio between PS-RAFT and MAC.
[c] PS-RAFT: acylated PS loading RAFT agent 0.92 mmol/g.
[d] Cationic PS: cationic PS using PS-RAFT[c] as a substrate.
[e] PS-RAFT: acylated PS loading RAFT agent 0.50 mmol/g.
[f] Cationic PS: cationic PS using PS-RAFT[e] as a substrate.

surrounded with transparency polymeric gel. The process is schematically represented in Figure 1. Weight increasing was evaluated by the following equation:

$$\Delta W\% = \frac{W_2 - W_1}{W_1} \times 100\% \quad (1)$$

Where ΔW is the weight increasing of PS-RAFT, W_2 is the weight of cationic PS spheres, and W_1 is the weight of PS-RAFT.

Characterizations

FT-IR spectrums of various PS spheres in KBr pellets were recorded by NEXUS 670 (Thermo Nicolet, USA), operating between 4000 and 400 cm^{-1}. The ^{13}C solid state NMR (400 MHz) spectra were obtained with a Bruker plus-400 (Bruker, Germany) spectrometer. The thermal stabilities were evaluated using thermal gravimetric analysis (TGA, Q500, TA, USA). Samples were heated in an aluminum crucible to 700°C at a heating rate of 10°C/min, whereas the apparatus was continually flushed with a nitrogen flow of 25 mL/min. The surface morphologies were observed using a scanning electron microscope (SEM, EVO18, ZEISS, Germany). Element analyses of cationic PS spheres were investigated by elemental analyzer (Vario EL cube, Elementar, Germany). The polyelectrolyte loading and RAFT loading were calculated by the following equations:

$$X_c = \frac{N\%}{14} \quad (2)$$

$$X_d = \frac{S\%}{32 \times 3} \quad (3)$$

Where X_c (mmol/g) is the polyelectrolyte loading of cationic PS spheres, X_d (mmol/g) is the RAFT loading of cationic PS spheres, N % is Nitrogen content of cationic PS spheres, S % is Sulfur content of cationic PS spheres, 14 is Nitrogen relative atomic mass, 32 is Sulfur relative atomic mass, 3 represents that each of RAFT agent has three sulfur atoms.

Determination of Model Contaminants

Analysis of the supernatant in PGA-containing samples was done by comparing the absorbance before and after adsorption with an Ultraviolet spectrophotometer (DR5000, Hatch Company, USA) according to a previously published method.[25] The amount of PGA, x (mg/L), was calculated according to the following equation:

$$y = 0.0091x - 0.0012 \quad (R^2 = 0.9922) \quad (4)$$

where y is the absorbance of the PGA solution.

Analysis of the supernatant in lignin-Na-containing samples was also done by DR5000 according to a literature method.[26] The amount of lignin-Na, x (mg/L), was calculated with the following equation:

$$y = 0.0075x + 0.1039 \quad (R^2 = 0.9972) \quad (5)$$

where y is the absorbance of the lignin-Na solution.

Model Contaminants Uptake Experiments

Batch adsorption experiments were conducted and equilibrated using a thermostatic shaker bath operated at 100 rpm at different temperature. All of the adsorption experiments were repeated at least twice to verify the results.

The adsorption isotherms were determined by placing dried cationic PS spheres (1.35 mmol/g poly-MAC loading) into a series of PGA or lignin-Na solutions (10 mL) with concentrations ranging from 10 mg/L to 500 mg/L. The residual PGA and lignin-Na concentration were determined at 60°C after 30 min adsorption process.

The adsorption kinetics were analyzed by placing dried cationic PS spheres into PGA solutions (100 mg/L, 100 mL) and lignin-Na solutions (300 mg/L, 100 mL). Samples were taken out at predetermined time intervals for the analysis of residual PGA or lignin-Na concentration in solutions.

RESULTS AND DISCUSSION

Generation of Cationic Polyelectrolyte Brushes on PS Spheres

Cross-linked polystyrene spheres with poly-MAC brushes were prepared by surface-initiated reversible addition-fragmentation

Table II. Effect of Initiate/Additional RAFT Mass Ratio on Preparation of Cationic PS Spheres (PS-RAFT Loading High RAFT Agent as a Substrate)

Samples[a]	Initiate/%	Additional RAFT/%	S %	N %	Weight increasing /%	RAFT loading (mmol/g)	Polyelectrolyte Loading (mmol/g)
PS-RAFT[b]	—	—	8.848	—	—	0.92	—
Cationic PS[c]	0.1	0	6.202	1.89	42.48	0.65	1.35
Cationic PS[c]	0.1	0.1	6.316	1.80	39.79	0.66	1.29
Cationic PS[c]	0.1	0.5	6.571	1.77	37.45	0.68	1.26
Cationic PS[c]	0.3	0	6.788	1.71	37.37	0.71	1.22
Cationic PS[c]	0.3	0.1	6.828	1.67	35.30	0.71	1.19
Cationic PS[c]	0.3	0.5	6.088	1.30	32.69	0.63	0.93

[a] Monomer (MAC) concentration: 30%, solvent: DMF, PS/MAC: 1 : 20, polymerization temperature:70°C, polymerization time: 12 h.
[b] PS-RAFT: acylated PS loading RAFT agent 0.92 mmol/g.
[c] Cationic PS: cationic PS using PS-RAFT[b] as a substrate.

chain transfer polymerization (SI-RAFT) of MAC. SI-RAFT has been widely used for creating dense polymer brushes on solid surfaces.[27,28] The crucial task in this strategy is the incorporation of RAFT as macro-CTA on the substrate surfaces. The most common approach is bonding a coupling agent containing sulphur ester on the solid substrate.[29,30] It is rare to bond sulfur ester onto the substrate without coupling agents. The use of acylated PS spheres loading RAFT agent as solid macro-CTA can be considered as a distinctive way to generate cationic polyelectrolyte linked to the bead cores.

The results of two types of cationic PS spheres with different amount of cationic polyelectrolyte were shown in Table I. It was found that the PS/MAC mass ratio had influenced on the weight increasing and polyelectrolyte loading. For the acylated PS with high content of RAFT (about 0.92 mmol/g), poly-MAC grafted onto the PS increased from 0.84 to 1.25 mmol/g (+49%). However, the acylated PS with low content of RAFT (about 0.50 mmol/g), poly-MAC grafted onto the PS increased only from 0.74 to 1.04 mmol/g (+41%). These results can be explained that polyelectrolyte loading had increased at the close rate whether the content of RAFT. But acylated PS spheres with higher content of RAFT had more initiation points, indicating that there were more active points to insert poly-MAC. On the other hand, with the increasing of MAC content, more MAC molecules had chances to get in touch with surface of PS spheres and chemically bonded on them, thus polyelectrolyte loading increased significantly.

To investigate the influences of initiator/RAFT mass ratio on the resulting characteristics of cationic PS spheres, two batches of polymerization were performed at fixed conditions (Tables II and III). The first batch of polymerization was prepared with acylated PS loading RAFT agent (0.92 mmol/g) as a substrate and the second batch was done with acylated PS loading RAFT agent (0.50 mmol/g). From Table II, it shows that the amounts of RAFT loading reduced from 0.92 mmol/g to about 0.67 mmol/g in different initiate/additional RAFT mass ratios. When the amount of initiator was 0.1%, poly-MAC grafting onto the PS reduced from 1.35 to 1.26 mmol/g (−6.7%) with the increase of RAFT. On the higher content of initiator (0.3%), poly-MAC declined from 1.22 to 0.93 mmol/g (−23.8%) with the increase of RAFT. Compared with Table II, cationic PS had less polyelectrolyte loading and RAFT agent loading in Table III. Polyelectrolyte loading ranged from 1.28 to 1.05 mmol/g (−18.0%) when the initiator was 0.1%. When the initiator increased to 0.3%, polyelectrolyte loading varied from 1.14 to 0.85 mmol/g (−25.4%). Additional RAFT agent could improve

Table III. Effect of Initiate/Additional RAFT Mass Ratio on Preparation of Cationic PS Spheres (PS-RAFT Loading low RAFT Agent as a Substrate)

Samples[a]	Initiate /%	Additional RAFT/%	S %	N %	Weight increasing/%	RAFT loading (mmol/g)	Polyelectrolyte Loading (mmol/g)
PS-RAFT[b]	—	—	4.806	—	—	0.50	—
Cationic PS[c]	0.1	0	3.338	1.79	44.20	0.35	1.28
Cationic PS[c]	0.1	0.1	3.263	1.62	37.90	0.34	1.16
Cationic PS[c]	0.1	0.5	3.478	1.47	28.65	0.36	1.05
Cationic PS[c]	0.3	0	3.561	1.60	33.97	0.37	1.14
Cationic PS[c]	0.3	0.1	3.898	1.30	23.64	0.41	0.93
Cationic PS[c]	0.3	0.5	3.78	1.19	19.81	0.39	0.85

[a] Monomer (MAC) concentration: 30%, solvent: DMF, PS/MAC: 1:20, polymerization temperature:70°C, polymerization time: 12 h.
[b] PS-RAFT: acylated PS loading RAFT agent 0.50 mmol/g.
[c] Cationic PS: cationic PS using PS-RAFT[b] as a substrate.

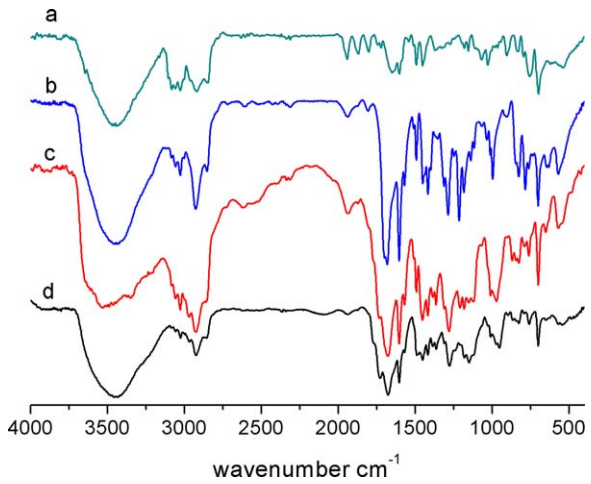

Figure 2. Fourier transformation infrared (FT-IR) spectra of PS spheres (a: PS, b: acylated PS, c: PS-RAFT, d: cationic PS). [Color figure can be viewed in the online issue, which is available at wileyonlinelibrary.com.]

the chain transfer polymerization and decrease the MAC grafting rate, causing to reduce the amount of poly-MAC grafting onto the PS. The more RAFT adding into the polymerization system, the more significant the chain transfer effect. Appropriate initiator concentration was 0.1% in which PS spheres could graft more poly-MAC regardless of the amount of RAFT.

Characteristics of PS Spheres with Cationic Polyelectrolyte Brushes

Obvious differences in wave numbers and intensities of the absorption bands can be observed between the spectra of PS and modified PS as shown in Figure 2. From all the spectra, the absorption bands at 1417 and 826 cm^{-1} were assigned to the methene ($-CH_2-$) asymmetric stretching vibration and the hydrocarbon bond (C–H) bending vibration of the benzene ring, respectively. Regarding to acylated PS, the peak at 1682 and 1286 cm^{-1} corresponded to carbonyl group (–C═O) and carbon chlorine bond (–CH_2–Cl), respectively, which were also

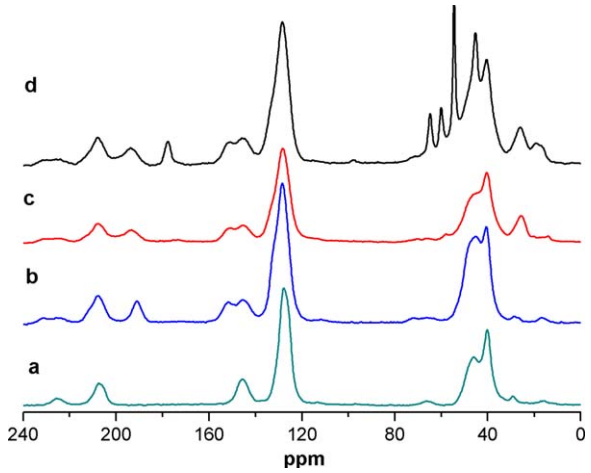

Figure 3. ^{13}C-NMR spectra of PS and modified spheres (a: PS, b: acylated PS, c: PS-RAFT, d: cationic PS). [Color figure can be viewed in the online issue, which is available at wileyonlinelibrary.com.]

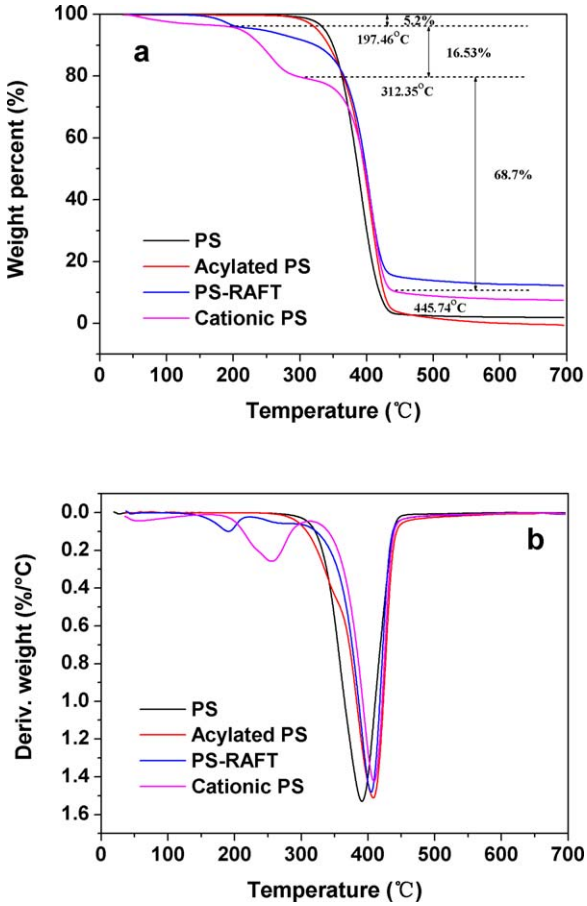

Figure 4. Thermogravimetric analysis for PS spheres and modified ones: (a) TGA and (b) DTGA. [Color figure can be viewed in the online issue, which is available at wileyonlinelibrary.com.]

observed from PS-RAFT and cationic PS. The band at 1733 cm^{-1} was characteristic of the ester bond (O═C–O) in PS-RAFT, which showed that RAFT agent had been successfully connected onto the acylated PS. Ester carbonyl group (O═C–O) stretching vibration was also observed in cationic PS that may be from RAFT agent or MAC. Another clear band at 952 cm^{-1} was attributed to the quaternary ammonium groups, which confirmed the MAC was bonded onto the PS-RAFT successfully.

The ^{13}C solid-state NMR spectra of PS and modified PS are showed in Figure 3. From Figure 3(a), the resonances with chemical shifts of about 40.2 and 45.9 ppm can be assigned to CH_2 and CH units in the PS backbone, respectively. In Figure 3(b), new peak of about 191 ppm can be assigned to ketone carbonyl, indicating that chloroacetyl chloride had been bonded onto the PS. In Figure 3(c), there were five new resonances with chemical shifts of about 14, 57.9, 65.3, 173.2, and 193.2 ppm, which were associated with –CH_3, –CH_2–N–, –CH_2–O–, ester carbonyl, ketone carbonyl, respectively. These indicated RAFT agent had been bonded to the acylated PS. In Figure 3(d), there were seven new resonances with chemical shifts of about 19.5, 54.4, 57.9, 60.1, 64.7, 177.7, and 193.6 ppm, which were associated with –CH_3, –CH_2–N–, –C–S–, quaternary carbon, –CH_2–

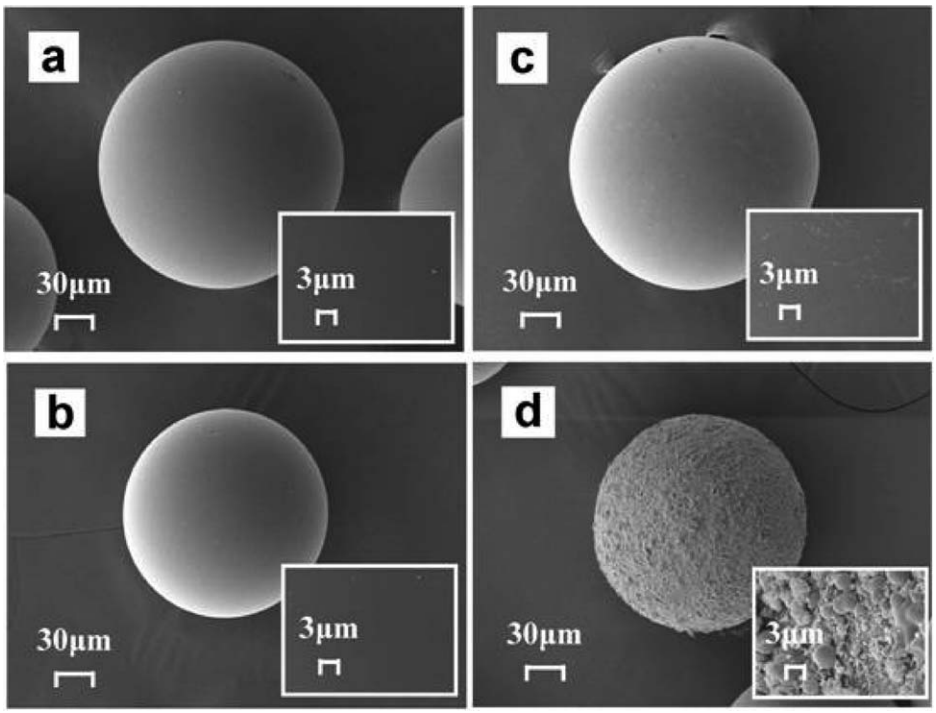

Figure 5. SEM images of PS spheres (a), acylated PS spheres (b), PS-RAFT spheres (c), and cationic PS spheres d).

O–, ester carbonyl, ketone carbonyl, respectively. These indicated that poly-MAC had been grafted onto the PS spheres.

Thermal gravimetric analysis of PS spheres and modified ones was conducted with TGA. Figure 4 gives the thermal gravimetric (TG) and derivative TG curves for various PS spheres with a heating rate of 10°C/min under a nitrogen atmosphere. For PS spheres, thermal degradation occurred in one distinct stage, and the maximum value of the peak (which characterizes the degradation of cross-linked PS), appeared at 391°C. Regarding to acylated PS spheres, the maximum value of the single peak shifted at 408°C because some benzene rings of PS had been substituted by chloroacetyl chloride. For acylated PS spheres loading some RAFT agent, the maximum value of the single peak had no big changes and appeared at 404°C. After grafting poly-MAC onto the PS spheres, two peaks appeared in derivative TG curves, with the main peak at 409°C and shoulder peak around 255°C. Three decomposition stages in the TG curve of cationic PS sphere were seen in Figure 4(a). The first weight loss (5.2%) was due to the residual and impurities from solvents and moisture. The second degradation started around 197°C and up to around 312°C, showing that about 16.53% of the product was degraded. The second weight loss could be attributed to the degradation of the linear poly-MAC layer. The last degradation took place at about 312 to 446°C, where about 68.70% of the product was degraded, corresponding to the degradation of the PS sphere core.

SEM images of PS spheres and modified ones are displayed in Figure 5. It can be seen that the surfaces of PS spheres and acylated PS spheres were smooth. Although the surfaces of PS-RAFT spheres became a little coarser comparing with PS spheres and acylated PS spheres, it is obvious that the surfaces of cationic PS spheres became rough after surface initiated RAFT of MAC from PS spheres (Figure 1). All of these results indicate that the poly-MAC was grafted from the surfaces of PS spheres successfully *via* the proposed SI-RAFT technique.

Adsorption of Model Contaminants on Cationic PS Spheres

The equilibrium adsorption isotherms are fundamental in describing the interaction between the adsorbent and adsorbate. The model contaminants (PGA and lignin-Na) adsorption isotherms for cationic PS are presented in Figure 6. Two common isotherm models for adsorption were used to fit experimental data in Table IV.

Langmuir isotherm model is based on the assumption that adsorption sites are identical and energetically equivalent, and

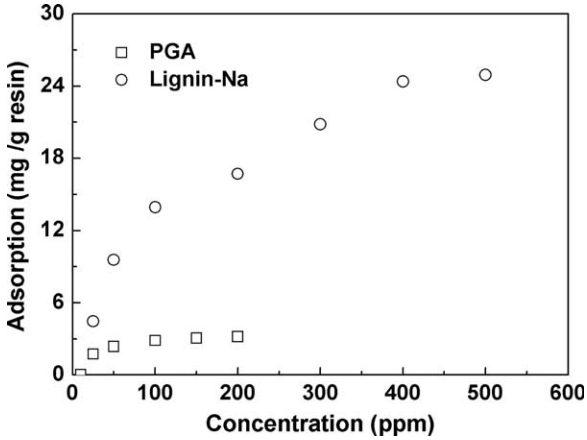

Figure 6. Adsorption isotherms of model contaminants.

Table IV. Isotherms Parameters of PGA and Lignin-Na Adsorption onto the Cationic PS

Model contaminants	Langmuir model			Freundlich model			Langmuir-Freundlich			
	k_L	a_L	R^2	a_F	b_F	R^2	k_{LF}	a_{LF}	b_{LF}	R^2
PGA	0.0918	0.0227	0.8864	0.3508	0.4345	0.7696	0.0013	0.00041	2.4175	0.9553
Lignin-Na	0.2293	0.0073	0.9749	1.5024	0.4589	0.9685	—	—	—	—

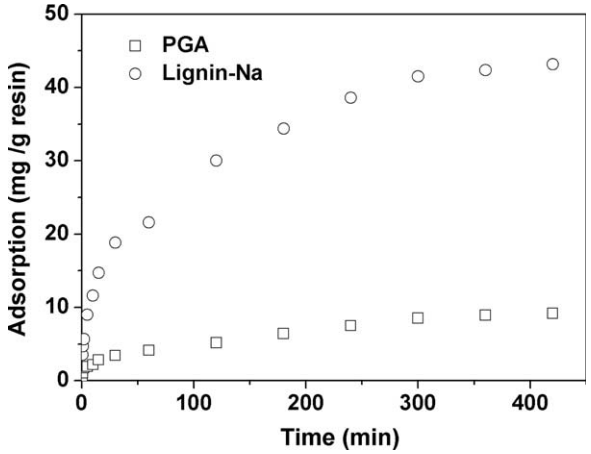

Figure 7. Adsorption kinetics of model contaminants.

only monolayer adsorption occurs in the process.[31] It is mathematically described as follows:

$$q_e = \frac{k_L C_e}{1 + a_L C_e} \tag{6}$$

Where q_e (mg/g) represents the amount of material adsorbed at adsorption equilibrium and Ce is the equilibrium adsorbent concentration. k_L and a_L are the corresponding parameters for isotherms.

Freundlich isotherm model is based on the assumption of exponentially decaying adsorption site energy distribution. It is used for heterogeneous surface energy systems and can be given as follows:[32]

$$q_e = a_F C_e^{\,b_F} \tag{7}$$

Where q_e (mg/g) represents the amount of material adsorbed at adsorption equilibrium and Ce is the equilibrium adsorbent concentration. a_F and b_F are the corresponding parameters for isotherms.

Langmuir-Freundlich isotherm model is based on the assumption that adsorption sites are identical and energetically equivalent, and only multilayer adsorption occurs in the process.[33] It is mathematically described as follows:

$$q_e = \frac{k_{LF} C_e^{\,b_{LF}}}{1 + a_{LF} C_e^{\,b_{LF}}} \tag{8}$$

Where q_e (mg/g) represents the amount of material adsorbed at adsorption equilibrium and C_e is the equilibrium adsorbent concentration. k_{LF}, a_{LF} and b_{LF} are the corresponding parameters for isotherms.

The theoretical isotherm parameters, k_L, a_L, a_F, b_F, k_{LF}, a_{LF}, b_{LF}, and R^2 are listed in Table IV. For PGA, the R^2 of the linear form for Langmuir-Freundlich model was much closer to unity than for other models. Regarding to lignin-Na, the R^2 of the linear form for Langmuir model was nearly the same with Freundlich model. From Figure 6, the nonlinear curve of PGA revealed that multilayer adsorption model such as Langmuir-Freundlich was generally the best to describe the adsorption of PGA on cationic PS. The curve of adsorption isotherms of lignin-Na represented differently from the PGA, as it was well described by the Langmuir model, which represented a monolayer adsorption. Cationic PS spheres could adsorb 24 mg lignin-Na/g after 30 min, whereas only adsorb 3 mg PGA/g. This suggested that lignin-Na had a greater affinity for cationic PS than PGA.

Figure 7 shows the kinetics of the adsorption of PGA and lignin-Na by the cationic PS spheres. To examine the mechanism of the adsorption process, the commonly used kinetic models: the pseudo-first-order, intra-particle diffusion models were used to examine the kinetics data. The pseudo-first-order [Eq. (9)] and intra-particle diffusion [Eq. (10)] are illustrated as follows:[34,35]

$$q_t = q_{e1} - \frac{q_{e1}}{e^{k_1 t}} \tag{9}$$

$$q_t = k_{id} t^{0.5} + C \tag{10}$$

where q_t (mg/g) is the amount of PGA or lignin-Na adsorbed onto cationic PS at time t (min). q_{e1} and k_1 are the parameters for kinetics of pseudo-first-order. k_{id}, and C are the parameters for kinetics of intra-particle diffusion.

Table V. Kinetic Parameters of PGA and Lignin-Na Adsorption onto the Cationic PS

Model contaminants	Pseudo-first-order			Intraparticle diffusion		
	q_{e1} (mg/g)	k_1 (min^{-1})	R^2	C (mg/g)	k_{id} (mg/(g $min^{0.5}$))	R^2
PGA	8.5316	0.0112	0.8824	0.7708	0.4265	0.9866
Lignin-Na	39.8591	0.0176	0.9201	4.6838	2.0769	0.9778

Upon inspection of the adsorption curves in Figure 7, it is shown that the adsorption rate of lignin-Na increased faster than that of PGA. And the adsorption quantity of lignin-Na was larger than PGA. As for lignin-Na and PGA, cationic PS could adsorb lignin-Na from 3.49 to 43.16 mg/g comparing with PGA only from 0.23 to 9.14 mg/g in 420 min. From Table V, nonlinear regression of these curves revealed that adsorption of PGA and lignin-Na on cationic PS was adequately described by the intraparticle diffusion model, which meant that intraparticle diffusion was the main parameter governing adsorption rate.

CONCLUSIONS

In conclusions, polystyrene spheres with cationic polyelectrolyte brushes (poly-MAC) were successfully synthesized by surface-initiated reversible addition-fragmentation chain transfer polymerization. FT-IR, ^{13}C-NMR, SEM, element analysis, TGA technique was verified that poly-MAC had bonded onto the surface of polystyrene spheres. Through comparative tests, polystyrene spheres could graft 1.35 mmol/g poly-MAC at the optimized conditions. The adsorption of PGA and lignin-Na on cationic PS spheres indicated that adsorption equilibrium isotherm of PGA followed Langmuir-Freundlich adsorption model with an adsorption capacity of 3 mg PGA/g and the adsorption isotherm of lignin-Na conformed to Langmuir adsorption model with an adsorption capacity of 24 mg lignin-Na/g. In addition, kinetic studies of PGA and lignin-Na adsorption on cationic PS spheres revealed that intraparticle diffusion function played the most important role in the adsorption process.

ACKNOWLEDGMENTS

The authors gratefully acknowledge the State Key Laboratory of Pulp and Paper Engineering Fund (No.201425) for its financial support.

REFERENCES

1. Hubbe, M. A.; Rojas, O. J.; Venditti, R. A. *Nord. Pulp. Pap. Res. J.* **2006**, *21*, 154.
2. Miao, Q. X.; Huang, L. L.; Chen, L. H. *Bioresources* **2013**, *8*, 1431.
3. Holbery, J. D.; Wood, D. L.; Fisher, R. M. *Tappi J.* **2000**, *83*, 1.
4. Vendries, E.; Pfromm, P. H. *Tappi J.* **1998**, *81*, 206.
5. Francis, D. W.; Ouchi, M. D. *J. Pulp Pap. Sci.* **2001**, *27*, 289.
6. Maher, L. E.; Stack, K. R.; Mclean, D. S.; Richardson, D. E. *Appita J.* **2007**, *60*, 112.
7. Esser, A.; Kobayash, K.; Hiuga, S. *Jpn. Tappi J.* **2005**, *59*, 52.
8. Kekkonen, J.; Lattu, H.; Stenius, P. *J. Pulp Pap. Sci.* **2002**, *28*, 6.
9. Carre, B.; Brun, J.; Galland, G. *Pulp Pap. Canada* **1998**, *9*, 75.
10. Hassler, T. *Tappi J.* **1988**, *71*, 195.
11. Nuortila-Jokinen, J.; Manttari, M.; Huuhilo, T.; Kallioinen, M.; Nystrom, M. *Water Sci. Technol.* **2004**, *50*, 217.
12. Liu, K.; Zhao, G. L.; He, B. H.; Chen, L. H.; Huang, L. L. *Bioresour. Technol.* **2012**, *123*, 616.
13. Loranger, E.; Daneault, C.; Chabot, B. *Chem. Eng. J.* **2010**, *160*, 671.
14. Loranger, E.; Daneault, C.; Chabot, B.; Vallerand, R. *Can. J. Chem. Eng.* **2010**, *88*, 12.
15. Moebius, C. H. *Water Sci. Technol.* **1981**, *13*, 681.
16. Veverka, P.; Jerabek, K. *React. Funct. Polym.* **1999**, *41*, 21.
17. Pan, B. C.; Xiong, Y.; Li, A. M.; Chen, J. L.; Zhang, Q. X.; Jin, X. Y. *React. Funct. Polym.* **2002**, *53*, 63.
18. Bayramoglu, G.; Altintas, B.; Arica, M. Y. *Chem. Eng. J.* **2009**, *152*, 339.
19. Ozer, O.; Ince, A.; Karagoz, B.; Bicak, N. *Desalination* **2013**, *309*, 141.
20. Guo, X.; Weiss, A.; Ballauff, M. *Macromolecules* **1999**, *32*, 6043.
21. Karagoz, B.; Bayramoglu, G.; Altintas, B.; Bicak, N.; Arica, M. Y. *Ind. Eng. Chem. Res.* **2010**, *49*, 9655.
22. Takolpuckdee, P.; Mars, C. A.; Perrier, S. *Org. Lett.* **2005**, *7*, 3449.
23. Lee, A.; Bütün, V.; Vamvakaki, M.; Armes, S. P.; Pople, J. A.; Gast, A. P. *Macromolecules* **2002**, *35*, 8540.
24. Lai, J. T.; Filla, D.; Shea, R. *Macromolecules* **2002**, *35*, 6754.
25. Yeoh, S.; Zhang, S.; Shi, J.; Langrish, T. A. G. *Chem. Eng. Commun.* **2008**, *195*, 511.
26. Sudekum, K. H.; Voigt, K.; Monties, B.; Stangassinger, M. *J. Agric. Food Chem.* **1997**, *45*, 1220.
27. Rzayev, Z. M. O.; Soylemez, E. A.; Davarcioglu, B. *Polym. Adv. Technol.* **2012**, *23*, 278.
28. Audouin, F.; Heise, A. *Eur. Polym. J.* **2013**, *49*, 1073.
29. Li, C. Z.; Benicewicz, B. C. *Macromolecules* **2005**, *38*, 5929.
30. Zhao, Y. L.; Perrier, S. *Macromolecules* **2007**, *40*, 9116.
31. Lieberman, M. A. *Plasma Sources Sci. Technol.* **2009**, *18*, 1.
32. Gessner, P. K.; Hasan, M. M. *J. Pharm. Sci.* **1987**, *76*, 319.
33. Haghtalab, A.; Nabipoor, M.; Farzad, S. *Fuel Process. Technol.* **2012**, *104*, 73.
34. Wong, Y. C.; Szeto, Y. S.; Cheung, W. H.; Mckay, G. *J. Appl. Polym. Sci.* **2004**, *92*, 1633.
35. Mirzajani, R.; Ahmadi, S.; Malakooti, R.; Mahmoodi, H. *J. Porous Mater.* **2014**, *21*, 413.